Accepted Manuscript

8-Br-quinoline derivatives as sensitizers combining two-photon induced fluorescence and singlet oxygen generation

Sébastien Picard, Guillaume Clermont, Emilie Genin, Mireille Blanchard-Desce

PII: S0040-4020(14)01800-6

DOI: 10.1016/j.tet.2014.12.084

Reference: TET 26305

To appear in: *Tetrahedron*

Received Date: 27 October 2014

Revised Date: 19 December 2014

Accepted Date: 23 December 2014

Please cite this article as: Picard S, Clermont G, Genin E, Blanchard-Desce M, 8-Br-quinoline derivatives as sensitizers combining two-photon induced fluorescence and singlet oxygen generation, *Tetrahedron* (2015), doi: 10.1016/j.tet.2014.12.084.

Graphical Abstract

To create your abstract, type over the instructions in the template box below.
Fonts or abstract dimensions should not be changed or altered.

8-Br-quinoline derivatives as sensitizers combining two-photon induced fluorescence and singlet oxygen generation.

Leave this area blank for abstract info.

Sébastien Picard, Guillaume Clermont, Emilie Genin, Mireille Blanchard-Desce*
Univ. Bordeaux, Institut des Sciences Moléculaires, CNRS UMR 5255, 351 cours de la Libération, F-33405 Talence Cedex, France

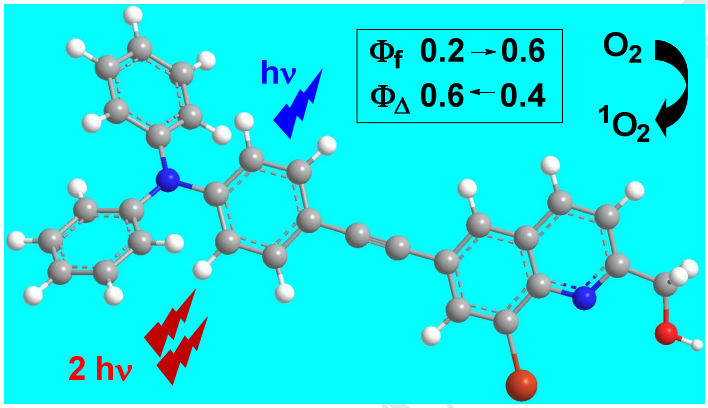

Tetrahedron
journal homepage: www.elsevier.com

8-Br-quinoline derivatives as sensitizers combining two-photon induced fluorescence and singlet oxygen generation.

Sébastien Picard, Guillaume Clermont, Emilie Genin, Mireille Blanchard-Desce*

Univ. Bordeaux, Institut des Sciences Moléculaires, CNRS UMR 5255, 351 cours de la Libération, F-33405 Talence Cedex, France

ARTICLE INFO

Article history:
Received
Received in revised form
Accepted
Available online

Keywords:
8-Br-quinolines
Friedländer reaction
Singlet oxygen production
Two-Photon Absorption
Fluorescence

ABSTRACT

The present study describes the synthesis of a series of original 8-Br-quinoline derivatives with an arylethynyl moiety at the C6 position, based on Friedländer and Sonogashira coupling key reactions. Investigation of their photophysical and two-photon absorption (2PA) properties reveals that these structures can lead to 2PA chromophores combining fluorescence and singlet oxygen generation properties. As a result, chromophores which combine significant 2PA responses in the NIR region, good photosensitization ability (Φ_Δ = 0.4-0.6) and fluorescence properties (Φ_f = 0.2-0.6) have been identified. These multifunctional derivatives hold promises as original dyes for combined two-photon imaging and photodynamic therapy.

1. Introduction

Singlet molecular oxygen ($^1O_2$) is known to play key roles in a lot of biological processes such as intracellular signaling mechanisms and reactions leading to cell death via apoptosis or necrosis.[1] Over the years a large number of research programs have thus been dedicated to the design of molecular tools allowing either the detection or the production of singlet oxygen, especially for applications in functional biological systems.[1-2] The more remarkable medical application of photosensitized $^1O_2$ generation is undoubtedly ~~the~~ photodynamic therapy (PDT) which has arisen as a powerful non-invasive medical technique used in oncology for the treatment of several cancers such as skin, head and neck, lung, oesophageal, prostate and bladder as well as in ophthalmology for the treatment of macular degeneration.[3] PDT benefits from its greater tolerance of repeated doses and localization of the light irradiation helping to reduce side effects in comparison with chemotherapy. More recently, combining two-photon (2P) excitation with PDT, particularly *in vivo*, has offered new perspectives and gained increasing popularity due to the advantages it provides in terms of intrinsic 3D resolution, increased penetration depth in tissues and reduced collateral (out of focus) photodamage.[4] However, photosensitizers currently approved or in clinical trials, including Photofrin® and Visudyne® built from a porphyrin scaffold, display low 2PA cross-sections in the near IR (700-900 nm), which significantly limits their use in 2P excited PDT because a very high laser excitation power is required.[5]

Therefore, this has prompted the quest for novel 2P singlet oxygen sensitizers combining large 2PA cross-sections (σ_2) in the near IR region and highly efficient singlet oxygen production. The molecular engineering is tricky as features providing a strong enhancement of 2PA ability generally tend to decrease the $^1O_2$ production quantum yield.[1-2,6] An additional challenge relies on keeping a subtle balance between the different excited state outcomes (fluorescence or $^1O_2$ production) to develop *dual-role* biphotonic chromophores allowing two-photon induced image-guided PDT (i.e *in-vivo* monitoring and localized treatment combined).[7] In recent years, a wide range of π-conjugated poly(hetero)aromatic 2P sensitizers with high 2PA cross-sections have been designed based on guidelines derived from structure-properties relationships of 2PA chromophores, including distyrylbenzenes and difuranonaphthalenes,[8] aromatic ketones,[9] squaraine derivatives,[10] porphyrazines and porphycenes,[8c,11] expanded porphyrins,[12] porphyrins oligomers,[13] supramolecular porphyrins assemblies[14] as well as banana-shaped biphotonic quadrupolar chromophores[15] and "semi-disconnected" multiporphyrin assemblies[16] (Fig. 1).

* Corresponding author. Tel.: +33 5 40 00 67 32; fax: +33 5 40 00 69 94. E-mail address: m.blanchard-desce@ism.u-bordeaux1.fr

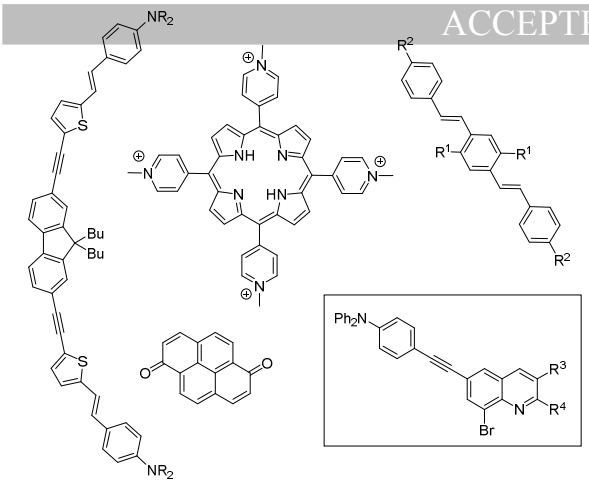

Fig. 1. Selected examples of reported 2P photosensitizers and chemical structure of the newly designed 8-bromo-quinoline derivatives (in the frame).

In this framework, we decided to investigate the potential of a new series of rather small organic molecules bearing a 8-bromo-quinoline moiety as two-photon fluorescent sensitizers. Quinoline derivatives are known to display a wide range of biological activities and pharmaceuticals properties such as antimalarial, antimicrobial, antibacterial, anti-Alzheimer, anti-HIV, and anticancer activity.[17] In contrast, only scarce reports mentioned the ability of mefloquine and quinine (well-known drugs used in the treatment of malaria) to produce singlet oxygen after excitation at 355 nm with quantum yields about 0.36 (in D_2O, pD 7) and, to the best of our knowledge, no systematic study has yet been conducted.[18] In the PDT research area, quinoline scaffolds are most commonly used as ligands to produce metal (Pt^{II}, Ru^{III}, Ir^{III}) complexes acting as efficient photosensitizers but the photosensitization properties originate primarily from the metal center.[19]

We herein describe our efforts towards the design of a new series of 8-Br-quinoline-based 2P photosensitizers displaying significant 2PA cross-sections in the NIR, combined with efficient singlet oxygen production and retaining fluorescence properties. To achieve this aim, we chose to extend quinoline scaffolds at the C6 position with a (diphenylamino)phenyl-ethynyl arm and to incorporate a bromine at the C8 position, as heavy atoms, when properly located, are known to facilitate intersystem crossing and consequently favor singlet oxygen generation.[1-2] Modulations at the C2 and/or C3 positions were explored. We thus report the first synthesis of 8-Br-quinoline derivatives functionalized at position C2 and/or C3. Our synthetic strategy is based on a Friedländer reaction to build the functionalized quinoline scaffold and on a Sonogashira cross-coupling reaction to graft the arylethynyl moiety. Photophysical and 2PA properties of the series of six chromophores were then investigated as well as their ability to generate singlet oxygen.

2. Results and discussion

2.1. Synthesis

Quinoline-based chromophores **6**, **10**, **12** were prepared from the key intermediate **5** by means of a Friedländer reaction with acetone or its derivatives (scheme 1).[20] The synthesis of the compound **5** was achieved following a two-step sequence starting from the known aldehyde **1**.[21] Bromination of aldehyde **1** with *N*-bromosuccinimide (NBS) afforded an inseparable mixture of compounds **2** and **3** (ratio 7:3, in 54% yield of **2**). Further one-pot two-step reaction, involving a Sonogashira cross-coupling / *in situ* TBAF promoted trimethylsilyl group deprotection, with alkyne **4** provided the derivative **5** as pure compound in a satisfactory 79% yield. Compound **6** was then obtained in almost quantitative yield from intermediate **5** by means of a Friedländer reaction with acetone, used as reagent and solvent, allowing building of the quinoline scaffold. Classical oxidation with selenium dioxide led to the aldehyde **7** with a moderate yield of 37%. Finally, the aldehyde was reduced into the corresponding alcohol with sodium borohydrate to afford alcohol **8** in excellent yield (Scheme 1).

As an alternative straightforward approach, we also studied the opportunity to obtain directly compound **8** by means of a Friedländer reaction between the intermediate **5** and the hydroxyacetone **9**. Strikingly, we did not observed the formation of the expected product **8** (performing TLC and NMR analysis of the crude) but we isolated the hydroxyquinoline derivative **10** in 50% yield (Scheme 1). The structure of the compound **10** (i.e the regiochemistry of the reaction) was confirmed by performing extensive spectroscopic analysis including NOESY experiments at 400 MHz in DMSO-d_6. Correlations between H4-H5 and H3-H4 were unambiguously observed and a weak NOE effect was also detected between H3-H2. We subsequently applied the Friedländer reaction to the dihydroxyacetone **11** to afford quinoline **12** in a moderate yield (Scheme 1). The production of hydroxyquinoline derivatives **10** and **12** can be explained considering the classical mechanism of the Friedländer reaction.[20] A dihydroquinoline intermediate bearing two hydroxyl groups at the C3 and C4 positions is formed and the regioselectivity of the process is further controlled by the final dehydration step (Scheme 2). The elimination of water follows the pathway (a), leading to the 3-hydroxy-quinoline regioisomer, since the proton at the C3 position (i.e α position from the imine function) is the more acidic.

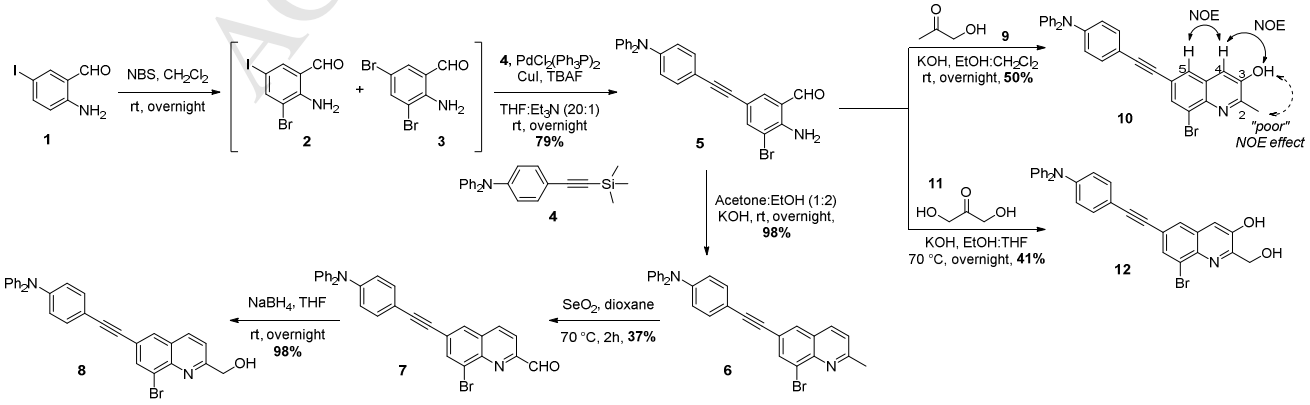

Scheme 1. Synthesis of the key intermediate **5** and quinolines **6**-**8**, **10** and **12**.

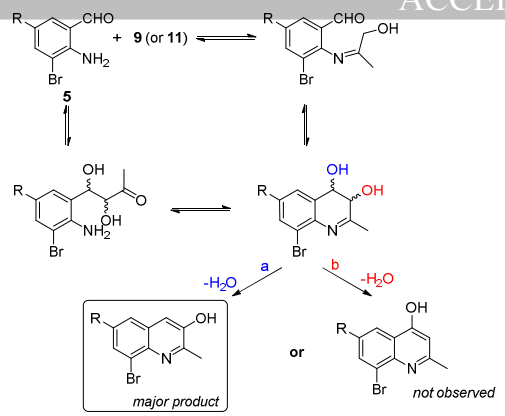

Scheme 2. Proposed mechanism of the Friedländer reaction leading to compounds **10** and **12**.

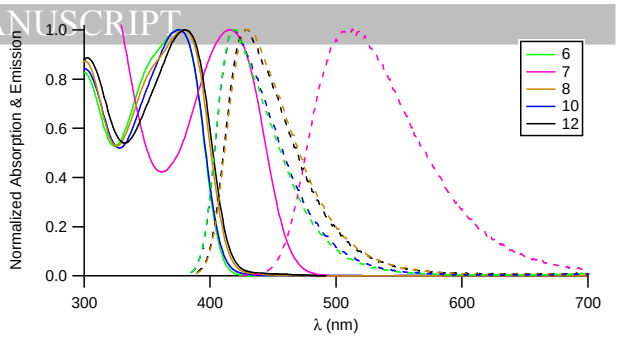

Fig. 2. Absorption (solid lines) and emission (dashed lines) spectra of quinolines **6-8**, **10**, **12** in toluene.

2.2. Photophysical properties

Photophysical properties (including one-photon absorption, fluorescence and singlet oxygen generation) of compounds **5-8**, **10** and **12** were investigated in toluene and the corresponding data are gathered in Table 1. All derivatives present an intense absorption band in the near UV-blue visible region with molar extinction coefficient values up to 3.9 x 10^4.M^{-1}.cm^{-1}. All quinolines (**6-8**, **10** and **12**) absorption spectra display two bands (Fig. 2): the low energy band can be ascribed to an intramolecular charge transfer (ICT) transition (see below) while the second band in the UV region (maximum around 300 nm) is characteristic of a higher energy π-π* transition. All quinolines compounds (**6-8**, **10** and **12**) also exhibit fluorescence in the violet to the green region (Fig. 2) with moderate (0.21) to high (0.68) quantum yields, whereas the fluorescence quantum yield of the aniline intermediate **5** is low. This confirms that the quinoline scaffold is crucial for providing significant fluorescence properties. From these data, we can also derive structure-properties relationships related to the modulations implemented at C2 and/or C3 positions. Replacing the methyl substituent at the C2 position by a hydroxymethyl moiety induces a slight hypochromic effect on the absorption as well as a bathochromic shift of the emission band and a slight decrease of the fluorescence quantum yield (consistent with an increase of the non-radiative decay rate). As expected, the introduction of the electron-withdrawing formyl group induces a large red-shift of both the absorption and emission bands and an increased Stokes' shift value, indicative of increased ICT character. Strikingly, a strong enhancement of the fluorescence properties is concomitantly observed (i.e. compound **7** displays the highest fluorescence quantum yield value, 0.60) due to a major decrease in non-radiative decay rate which overcomes the slightly lower radiative decay rate. In contrast, the presence of the hydroxyl group at the C3 position does not affect the absorption and emission properties of the quinoline-based chromophores, while it offers interesting possibilities for further covalent functionalization (such as grafting of targeting units).

The influence of the environment was investigated by studying the absorption and emission properties of the chromophores in organic solvents of increasing polarities (toluene, dichloromethane and acetonitrile). Intermediate **5** and quinolines **6**, **8**, **10**, **12** display a positive solvatochromic behavior (Fig. 3 and Fig. S1): increasing the solvent polarity does not greatly affect ~~much~~ the absorption band, while a marked red-shift of the emission band from violet-blue (in toluene) to yellow-orange (in acetonitrile) is observed. These features are typical of ICT transitions associated with an increase of dipole moment upon excitation, leading to polar emissive excited-states.

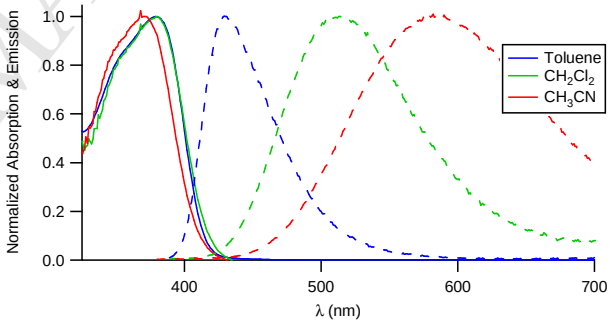

Fig. 3. Absorption (solid lines) and emission (dashed lines) spectra of compound **8** in solvents of different polarities.

The photosensitization and singlet oxygen generation properties were studied by measuring the $^1O_2$ luminescence at 1272 nm in toluene by comparison with a tetraphenylporphyrin (TPP) reference solution measured in the same solvent. The values of the singlet oxygen quantum yield (Φ_Δ) are collected in Table 1. Strikingly, all quinolines (**6-8**, **10** and **12**) display significant Φ_Δ values (varying from 0.4 to 0.6). The significantly lower singlet oxygen quantum yield of intermediate **5** (0.12) reveals the major importance of the quinoline feature at providing the photosensitization ability.

Table 1. Photophysical and 2PA characteristics of the intermediate **5** and quinolines **6-8**, **10**, **12** in toluene.

	λ_{abs}^{max} [nm]	ε^{max} [10^4.M^{-1}.cm^{-1}]	λ_{em}^{max} [nm]	Stokes' shift [10^3 cm^{-1}]	Φ_f [a]	τ [ns] [b]	k_r [10^8 s^{-1}] [c]	k_{nr} [10^8 s^{-1}] [c]	Φ_Δ [d]	λ_{2PA}^{max} [nm]	σ_2^{max} [GM]
5	354	3.9	408	3.7	0.03	1.1	0.3	8.8	0.12	/	/
6	375	3.3	419	2.8	0.27	0.6	4.4	12.0	0.53	760	116
7	416	2.3	511	4.5	0.60	2.2	3.0	1.5	0.40	830	265
8	379	2.7	431	3.2	0.21	0.6	3.5	13.2	0.62	770	154
10	375	3.4	419	2.8	0.26	0.6	4.3	12.3	0.43	750	120
12	380	2.6	429	3.0	0.21	0.5	4.0	15.0	0.57	760	157

[a] Fluorescence quantum yield determined relative to quinine in H_2SO_4 0.5M (Φ = 0.546) or fluorescein in 0.1M aqueous NaOH (Φ = 0.90).
[b] Fluorescence lifetime determined using time-correlated single-photon counting.
[c] Radiative (k_r) and non-radiative (k_{nr}) decay rates.

[d] Singlet oxygen quantum yield determined relative to tetraphenylporphyrin in toluene (Φ_Δ[TTP] = 0.68 in toluene)[22]

The substituents on the quinoline ring influence significantly the photosensitization ability. While the presence of the hydroxyl substituent at the C3 position of the quinoline scaffold induces a slight decrease (by less than 20%) of the photosensitization properties but does not affect the fluorescence efficiencies (comparison of quinolines **6**/**10** and **8**/**12** in Table 1), the substitution of one hydrogen of the methyl group at the C2 position by a hydroxyl moiety leads to an enhancement of the singlet oxygen production by about 20-30% and slight decrease of fluorescence efficiencies (comparison of quinolines **6**/**8** and **10**/**12** in Table 1). Hence the highest Φ_Δ value is obtained for quinoline **8** (0.62, which is close to that of the prototypical sensitizer TPP) while its fluorescence quantum yield is about twice larger. Strikingly, quinoline **7** bearing a formyl substituent at the C2 position maintains a satisfactory singlet oxygen quantum yield (albeit reduced of about 25% compared to compound **6**) while it shows both the most intense and red-shifted fluorescence emission (Table 1). For this compound, the excitation energy seems to be totally redistributed between the emission process and the $^1O_2$ generation.

2.3. Two-photon absorption (2PA)

Taking advantage of the fluorescent properties of the synthesized quinoline derivatives **6**-**8**, **10**, **12** in toluene, their 2PA properties in the NIR range (700-1000 nm) could be determined by using the two-photon induced fluorescence technique.[23] Maximum 2PA wavelengths and cross-section values are collected in Table 1 while 2PA spectra are shown in Fig. 4. As observed from Fig. 4, all derivatives display a broad 2PA band in the NIR region located at almost twice the wavelength of the one-photon absorption band (Fig. S2). This is consistent with the fact that the lowest-energy excited state is both one- and two-photon allowed. 2PA bands of compounds **6**, **8**, **10**, **12** peak at 750-770 nm with corresponding maximum 2PA cross-sections in the 120-155 GM range.

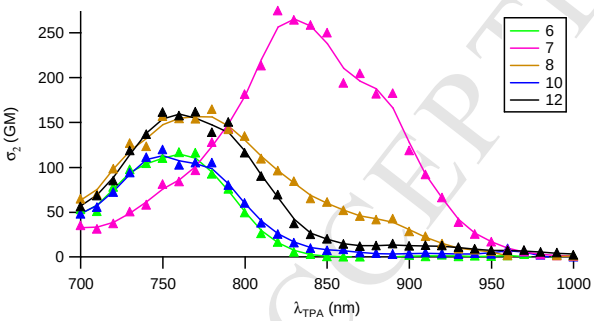

Fig. 4. 2PA spectra of compounds **5**-**8**, **10**, **12** in toluene.

While the introduction of the hydroxyl group at the C3 position does not affect the 2PA response, the presence of the hydroxymethyl appendices at the C2 position leads to an increase (by a factor 30%) of the 2PA cross-section, confirming our previous reports.[24] Finally, the presence of an electron-withdrawing formyl substituent at the C2 position is clearly enhancing the peak 2PA response as well as red-shifting the 2PA band (Fig. 4). Thus, quinoline derivative **7** displays the most interesting 2PA characteristics including a red-shifted 2PA band with a maximum at 830 nm and the largest peak 2PA response (265 GM).

Since the lowest excited state is both one-and two-photon allowed, the same (lowest-energy) excited state is reached when conducting two-photon excitation in the *lowest* 2PA band located in the NIR region. We can thus posit that the subsequent photochemistry (including intersystem crossing leading to the sensitiser triplet state liable to transfer its energy to molecular oxygen transfer in solution to produce reactive singlet oxygen) is the same. Hence in the case of the quinoline derivatives investigated in the present work, the Φ_Δ values can also be used for the calculation of σ_2^{max} Φ_Δ values for 2P excitation in the NIR range.

In summary, chromophores **7** and **8** meet all the prerequisites (suitable fluorescence and photosensitization properties combined with substantial 2PA responses, leading to σ_2^{max} Φ_Δ values of about 100 GM) for their use as sensitizers for *dual* PDT / fluorescence imaging induced by 2P excitation in the biological spectral window. As such they represent attractive molecular subunits for further incorporation in nano-objects that would be used as 2P nanotools for theranostics in the NIR range.[25]

3. Conclusion

A new family of 8-Br-quinolines derivatives with a (diphenylamino)phenyl-ethynyl moiety at the C6 position and incorporating modulations at the C2 position was efficiently prepared by applying a multistep synthetic route based on Friedländer and Sonogashira coupling key reactions. Very interestingly, all chromophores display rather large 2PA responses (σ_2^{max} values ranging from 116 to 265 GM) in the spectral range of interest for biological applications combined with high singlet oxygen production ability (Φ_Δ up to 0.62) while maintaining reasonable fluorescence properties. The present study thus validates our molecular engineering and demonstrates the potential of the original quinoline scaffold for the development of *dual role* two-photon sensitizers. Hence such derivatives offer major promises for image-guided therapy induced by 2P excitation (i.e. combined two-photon imaging and localized singlet oxygen generation). Moreover, the hydroxyl grafting moieties located at the C2 and/or C3 positions interestingly provides an easy way for subsequent functionalization. We are currently exploring the synthesis of more hydrophilic 8-Br-quinoline-based derivatives as well as the preparation of graftable analogs for their further incorporation within nanoparticles and/or their bio-conjugation with targeting units.

4. Experimental section

4.1. Synthetic procedures

4.1.1. *General methods.*

Solvents were freshly distilled before use over CaH_2 (for CH_2Cl_2 and Et_3N) or benzophenone/Na (for THF). Reactions were monitored by thin-layer chromatography carried out on silica gel precoated aluminium sheets (60F-254). Column chromatography was performed on Fluka silica gel 60 (40-63 µm). Melting points were measured on a Stuart SMP 10. Infrared spectra were measured on a Perkin Elmer Spectrum 100 Optica. ^1H and ^{13}C NMR spectra were recorded on a Bruker Advance III 200 spectrometer at 200 MHz and 50 MHz, respectively, and on a Bruker Advance III 600 spectrometer at 600 MHz. Shifts (δ) are given in parts per million with respect to solvent residual peak and coupling constant (J) are given in Hertz. LC/MS analyses were performed on a Shimadzu LCMS-2020. HMRS

spectra were performed by the CESAMO (Bordeaux, France) on a QStar Elite mass spectrometer (Applied Biosystems). The instrument is equipped with an ESI source and spectra were recorded in the negative/positive mode. The electrospray needle was maintained at 4500 V and operated at room temperature. Samples were introduced by injection through a 20 µL sample loop into a 400 µL/min flow of methanol from the LC pump. Elemental Analyses were carried out by the ″Institut de Chimie des Substances Naturelles″ (Gif-sur-Yvette, France).

*4.1.2. 2-Amino-3-bromo-5-iodobenzaldehPyde (**2**) and 2-amino-3,5-dibromobenzaldehyde (**3**).*

To a solution of 2-amino-5-iodobenzaldehyde[21] **1** (1.64 g, 6.64 mmol), in dry CH_2Cl_2 (40 mL), at room temperature, was added NBS (1.18 g, 6.64 mmol). The reaction mixture was stirred overnight at room temperature, quenched with a $Na_2S_2O_3$ solution and then extracted with dry CH_2Cl_2. The combined organic layer was washed with a saturated aqueous Na_2CO_3 solution, dried (Na_2SO_4) and then concentrated under reduced pressure. The crude was purified by a short column of silica gel (30% CH_2Cl_2 in petroleum ether) to give 1.58 g of an inseparable mixture of **2** (59%) and **3** (34%).

*4.1.3. 2-Amino-3-bromo-5-((4-(diphenylamino)-phenyl)ethynyl)benzaldehyde (**5**).*

To a solution of *N*,*N*-diphenyl-4-((trimethylsilyl)-ethynyl)aniline **4** (690 mg, 2.0 mmol), 2-amino-3-bromo-5-iodobenzaldehyde **2** (717 mg, 2.2 mmol), CuI (15.2 mg, 80 µmol), and $PdCl_2(Ph_3P)_2$ (28.1 mg, 40 µmol), in a dry mixture of THF:Et_3N (20:1, 21 mL), at room temperature, was dropwise added a solution of TBAF (1 M in THF, 2.2 mL, 2.2 mmol). The reaction mixture was stirred overnight at room temperature and then filtrated through Celite®. The filtrate was quenched with a saturated aqueous NH_4Cl solution and then extracted with CH_2Cl_2. The combined organic layer was dried (Na_2SO_4), and concentrated under reduced pressure. The crude was purified on silica gel (40% CH_2Cl_2 in petroleum ether) to give **5** (736 mg, 79%) as a yellow powder: melting point: 246 °C; ν_{max}(solid): 3468, 3324, 2737, 1672, 1609, 1571, 1528, 1485 cm^{-1}; ^{1}H NMR (200 MHz, $CDCl_3$) δ (ppm): 6.83 (br s, 2H), 6.96-7.16 (m, 8H), 7.22-7.38 (m, 6H), 7.66 (d, *J*=1.8 Hz, 1H), 7.78 (d, *J*=1.8 Hz, 1H), 9.81 (s, 1H); ^{13}C NMR (50 MHz, $CDCl_3$) δ (ppm): 86.5, 89.0, 109.9, 112.5, 115.9, 119.1, 122.4, 123.7, 125.2, 129.5, 132.5, 138.5, 140.3, 146.5, 147.3, 148.1, 192.8; ESIHMRS: $C_{27}H_{19}BrN_2O$ calculated for $[M]^+$: 466.0675, found 466.0658; elemental analysis: calculated for $C_{27}H_{19}BrN_2O+1/3H_2O$: C, 68.51; H, 4.19; N, 5.92; found: C, 68.51; H, 4.11; N, 5.65.

*4.1.4. 4-((8-Bromo-2-methylquinolin-6-yl)ethynyl)-N,N-diphenylaniline (**6**).*

To a solution of **5** (660 mg, 1.41 mmol), in acetone:EtOH (absolute) mixture (1:2, 15 mL), was added KOH (120 mg, 2.12 mmol). The reaction mixture was stirred overnight at room temperature, and then concentrated under reduced pressure. The residue was quenched with a saturated aqueous NH_4Cl solution and then extracted with CH_2Cl_2. The combined organic layer was dried (Na_2SO_4), and concentrated under reduced pressure. The crude was purified by a short column of silica gel (toluene as eluent) to give **6** (674 mg, 98%) as a white powder: melting point: 147 °C; ν_{max}(solid): 3039 2213, 1583, 1502, 1482, 1447 cm^{-1}; ^{1}H NMR (200 MHz, $CDCl_3$) δ (ppm): 2.81 (s, 3H), 6.97-7.17 (m, 8H), 7.27-7.43 (m, 7H), 7.88 (d, *J*=1.6 Hz, 1H), 7.98 (d, *J*=8.5 Hz, 1H), 8.12 (d, *J*=1.6 Hz, 1H); ^{13}C NMR (50 MHz, $CDCl_3$) δ (ppm): 25.9, 87.2, 91.7, 115.3, 121.8, 122.1, 123.5, 123.9, 124.2, 125.3, 127.4, 129.6, 130.3, 132.8, 135.5, 136.6, 147.2, 148.5, 161.0; ESIHMRS: $C_{30}H_{21}BrN_2$ calculated for $[M+H]^+$: 489.0960, found 489.0964; elemental analysis: calculated for $C_{30}H_{21}BrN_2$: C, 73.62; H, 4.32; N, 5.72; found: C, 73.43; H, 4.36; N, 5.67.

*4.1.5. 8-Bromo-6-((4-(diphenylamino)phenyl)-ethynyl)quinoline-2-carbaldehyde (**7**).*

A mixture of **6** (650 mg, 1.30 mmol), and selenium dioxide (174 mg, 1.56 mmol), in dioxane (10 mL) was heated at 70 °C for 2 h. The reaction mixture was cooled at room temperature, filtrated trough Celite®, and the filtrate was concentrated under reduced pressure. The crude was purified on silica gel (40% toluene in petroleum ether) to give **7** (240 mg, 37%) as an orange powder: melting point: 169 °C; ν_{max}(solid): 3070, 2921, 2849, 2196, 1707, 1586, 1488, 1327, 1269 cm^{-1}; ^{1}H NMR (200 MHz, $CDCl_3$) δ (ppm): 6.98-7.17 (m, 8H), 7.24-7.43 (m, 6H), 7.98 (d, *J*=1.5 Hz, 1H), 8.08 (d, *J*=8.4 Hz, 1H), 8.21-8.29 (m, 2H), 10.29 (s, 1H); ^{13}C NMR (50 MHz, $CDCl_3$) δ (ppm): 87.0, 94.3, 114.5, 118.8, 121.8, 124.1, 125.5, 125.7, 126.1, 129.6, 130.0, 131.1, 133.0, 136.6, 137.7, 144.5, 147.1, 149.0, 153.2, 193.3; ESIHMRS: $C_{30}H_{19}BrN_2O$ calculated for $[M+Na]^+$: 525.0572, found 525.0580.

*4.1.6. (8-Bromo-6-((4-(diphenylamino)phenyl)-ethynyl)quinolin-2-yl)methanol (**8**).*

To a solution of **7** (70.0 mg, 140 µmol), in dry THF (2 mL), at room temperature, was added $NaBH_4$ (10.6 mg, 280 µmol). The reaction mixture was stirred overnight at room temperature, quenched with a saturated aqueous NH_4Cl solution and then extracted with EtOAc. The combined organic layer was dried (Na_2SO_4) and then concentrated under reduced pressure. The crude was purified on silica gel (20% EtOAc in petroleum ether) to give **8** (69.4 mg, 98%) as a yellow powder: melting point: 146 °C; ν_{max}(solid): 3458, 3059, 3035, 2204, 1757, 1579, 1484, 1266 cm^{-1}; ^{1}H NMR (200 MHz, $CDCl_3$) δ (ppm): 4.56 (t, *J*=4.5 Hz, 1 H), 4.96 (d, *J*=4.5 Hz, 2H), 6.98-7.17 (m, 8H), 7.25-7.43 (m, 7H), 7.92 (d, *J*=1.8 Hz, 1H), 8.08 (d, *J*=8.5 Hz, 1H), 8.15 (d, *J*=1.8 Hz, 1H); ^{13}C NMR (50 MHz, $CDCl_3$) δ (ppm): 64.3, 87.0, 92.3, 115.1, 119.8, 122.0, 122.8, 124.0, 124.2, 125.4, 128.5, 129.6, 130.2, 132.8, 135.9, 137.1, 143.1, 147.2, 148.6, 160.5; ESIHMRS: $C_{30}H_{21}BrN_2O$ calculated for $[M+Na]^+$: 527.0729, found 527.0726; elemental analysis: calculated for $C_{30}H_{21}BrN_2O$: C, 71.29; H, 4.19; N, 5.54; found: C, 71.04; H, 4.32; N, 5.13.

*4.1.7. 8-Bromo-6-((4-(diphenylamino)phenyl) ethynyl)-2-methylquinolin-3-ol (**10**).*

To a solution of **5** (70 mg, 149 µmol), in a mixture of **9**:EtOH:CH_2Cl_2 (v:v:v, 1:1:1, 3 mL), at room temperature, was added KOH (12.6 mg, 225 µmol). The reaction mixture was stirred overnight at room temperature, and then concentrated under reduced pressure. The residue was quenched with a saturated aqueous NH_4Cl solution and then extracted with CH_2Cl_2. The combined organic layer was dried (Na_2SO_4) and then concentrated under reduced pressure. The crude was purified on silica gel (20% EtOAc in petroleum ether) to give **11** (40.0 mg, 50%) as a brown powder: melting point: 186 °C; ν_{max}(solid): 3027, 2207, 1586, 1505, 1491, 1419, 1370 cm^{-1}; ^{1}H NMR (600 MHz, DMSO-d_6) δ (ppm): 2.57 (s, 3H), 6.92 (d, *J*=8.6 Hz, 2H), 7.10 (t, *J*=7.7 Hz, 4H), 7.14 (t, *J*=7.4 Hz, 2H), 7.37 (t, *J*=7.7 Hz, 4H), 7.45 (d, *J*=8.6 Hz, 2H), 7.48 (s, 1H), 7.88 (s, 1H), 8.01 (s, 1H), 10.74 (s, 1H); ^{13}C NMR (50 MHz, DMSO-d_6) δ (ppm): 20.5, 87.3, 90.9, 114.1, 114.2, 120.5, 120.9, 123.2, 124.2, 125.0, 125.1, 129.0, 129.6, 129.8, 130.8, 132.6, 137.6, 146.3, 147.9, 151.0, 154.1; LC-MS: $C_{30}H_{21}N_2O$ calculated for $[M + H]^+$: 505.09, found 504.95 and $[M - H]^-$: 503.07, found 502.90.

*4.1.8. 8-Bromo-6-((4-(diphenylamino)phenyl)-ethynyl)-2-(hydroxymethyl)quinolin-3-ol (**12**).*

A mixture of dihydroxyacetone **11** (500 mg), in absolute EtOH (2 mL), was heated at 70 °C until a clear colorless solution was obtained. At this temperature, a solution of **5** (50 mg, 107 µmol) in dry THF (1 mL) was added and then KOH (12.0 mg, 214 µmol) was added. The reaction mixture was heated overnight at 70 °C, cooled at room temperature and then 20 mL of CH_2Cl_2 were added. The mixture was filtrated trough Celite® and the filtrate was concentrated under reduced pressure. The crude was purified on silica gel (30% EtOAc in petroleum ether) to give **12** (22.0 mg, 41%) as a brown powder: ν_{max}(solid): 3035, 2196, 1579, 1484, 1413, 1270, 1037, 748 cm^{-1}; ^1H NMR (200 MHz, DMSO-d_6) δ (ppm): 4.75 (d, *J*=4.5 Hz, 2H) , 5.01 (t, *J*=3.7 Hz, 1H), 6.92 (d, *J*=8.5 Hz, 2H), 6.98-7.17 (m, 6H), 7.57-7.29 (m, 7H), 7.93 (d, *J*=1.4 Hz, 1H), 8.06 (d, *J*=1.4 Hz, 1H), 10.87 (s, 1H); ^{13}C NMR (50 MHz, DMSO-d_6) δ (ppm): 60.8, 87.2, 91.3, 114.0, 115.4, 120.9, 121.2, 123.4, 124.2, 124.3, 125.2, 129.1, 129.8, 130.0, 131.1, 132.7, 146.3, 148.0, 150.3, 154.6; LC-MS: $C_{30}H_{21}N_2O_2$ calculated for $[M + H]^+$: 521.08, found 520.80 and $[M - H]^-$: 519.07, found 518.70.

4.2. Photophysical studies

All photophysical studies were performed with freshly-prepared air-equilibrated solutions at room temperature (298 K). UV/Vis absorption spectra were recorded on a Jasco V-670 spectrophotometer. Steady-state and time-resolved fluorescence measurements were carried out on a Fluorolog spectrofluorometer. Fully corrected emission spectra were obtained under excitation at the wavelength of the absorption maximum. Fluorescence quantum yields of dilute solutions were measured according to literature procedures using quinine bisulfate in H_2SO_4 0.5M (Φ = 0.546 at 347 nm) or fluorescein in 0.1M aqueous NaOH (Φ = 0.90 at 474 nm).[26] The reported fluorescence quantum yield values obtained via this method are within ±0.02. Fluorescence decays were measured in a time-correlated single photon counting (TCSPC) configuration, under excitation from selected nanoLED (370 nm). The instrument response was determined by measuring the light scattered by a Ludox suspension. The lifetime values were obtained from the reconvolution fit analysis of the decay profiles; the quality of the fits was judged by the reduced χ^2 value (χ^2 <1.1). The reported lifetimes are within ±0.1ns. Measurements of singlet oxygen quantum yield (Φ_Δ) were performed on a Fluorolog-3 (Horiba Jobin Yvon), using a 450 W Xenon lamp. The emission at 1272 nm was detected using a liquid nitrogen-cooled Ge-detector model (EO-817L, North Coast Scientific Co). Singlet oxygen quantum yields Φ_Δ were determined in toluene solutions, using tetraphenylporphyrin (TPP) in toluene as reference solution (Φ_Δ [TPP] = 0.68 in toluene[22]) and were estimated from $^1O_2$ luminescence at 1272 nm.

4.3. Two-photon absorption experiments

Two-photon absorption cross sections (σ_2) were determined from the two-photon excited fluorescence (TPEF) cross sections ($\sigma_2\Phi$) and the fluorescence emission quantum yield (Φ). TPEF cross sections were measured relative to fluorescein in 0.01M aqueous NaOH in the 680-1080 nm spectral range,[23,27] using the method described by Xu and Webb[23] and the appropriate solvent-related refractive index corrections.[28] The quadratic dependence of the fluorescence intensity on the excitation power was checked at all wavelengths. Measurements were conducted using an excitation source delivering fs pulses. This allows avoiding excited-state absorption during the pulse duration, a phenomenon which has been shown to lead to overestimated two-photon absorption cross-section values. To scan the 680-1080 nm range, a Nd:YVO4-pumped Ti:sapphire oscillator was used generating 140fs pulses at a 80 MHz rate. The excitation was focused into the cuvette through a microscope objective (10X, NA 0.25). The fluorescence was detected in epifluorescence mode via a dichroic mirror (Chroma 675dcxru) and a barrier filter (Chroma e650sp-2p) by a compact CCD spectrometer module BWTek BTC112E. Total fluorescence intensities were obtained by integrating the corrected emission. The experimental uncertainty of the absorption cross-section values determined from this method has been estimated to be ±10%.

Acknowledgments

MBD gratefully thanks the Conseil Régional d'Aquitaine for generous funding (Chaire d'Accueil grant). Partial funding from Agence Nationale pour la Recherche (Grants ANR-10-NANO-022-01 and ANR-10-BLAN-1436) is also acknowledged.

Supplementary Material

^1H and ^{13}C NMR spectra of all new compounds, solvatochromic data and 2PA data are available free of charge.

References and notes

1. Ogilby, P. R. *Chem. Soc. Rev.* **2010,** *39*, 3181-3209.
2. (a) Arnbjerg, J.; Johnsen, M.; Ogilby, P. R. *Spectrum* **2008,** *21*, 20-27; (b) Pedersen, S. K.; Holmehave, J.; Blaikie, F. H.; Gollmer, A.; Breitenbach, T.; Jensen, H. H.; Ogilby, P. R. *J. Org. Chem.* **2014,** *79*, 3079-3087.
3. (a) Oleinick, N. L.; Morris, R. L.; Belichenko, I. *Photochem. Photobiol. Sci.* **2002,** *1*, 1-21; (b) Dougherty, T. J. *J. Clin. Laser Med. Surg.* **2002,** *20*, 3-7; (c) Triesscheijn, M.; Baas, P.; Schellens, J. H. M.; Stewart, F. A. *Oncologist* **2006,** *11*, 1034-1044; (d) Robertson, C. A.; Evans, D. H.; Abrahamse, H. *J. Photochem. Photobiol. B* **2009,** *96*, 1-8; (e) Allison, R. R.; Sibata, C. H. *Photodiag. Photodyn. Ther.* **2010,** *7*, 61-75; (f) Phillips, D. *Pure Appl. Chem.* **2011,** *83*, 733-748.
4. (a) Bhawalkar, J. D.; Kumar, N. D.; Zhao, C. F.; Prasad, P. N. *J. Clin. Laser Med. Surg.* **1997,** *15*, 201-204; (b) Kim, S.; Ohulchanskyy, T. Y.; Pudavar, H. E.; Pandey, R. K.; Prasad, P. N. *J. Am. Chem. Soc.* **2007,** *129*, 2669-2675; (c) Brown, S. *Nat. Photonics* **2008,** *2*, 394-395; (d) Collins, H. A.; Khurana, M.; Moriyama, E. H.; Mariampillai, A.; Dahlstedt, E.; Balaz, M.; Kuimova, M. K.; Drobizhev, M.; YangVictor, X. D.; Phillips, D.; Rebane, A.; Wilson, B. C.; Anderson, H. L. *Nat. Photonics* **2008,** *2*, 420-424; (e) Starkey, J. R.; Rebane, A. K.; Drobizhev, M. A.; Meng, F.; Gong, A.; Elliott, A.; McInnerney, K.; Spangler, C. W. *Clin. Cancer Res.* **2008,** *14*, 6564-6573; (f) Khurana, M.; Moriyama, E. H.; Mariampillai, A.; Samkoe, K.; Cramb, D.; Wilson, B. C. *J. Biomed. Opt.* **2009,** *14*, 064006; (g) Gary-Bobo, M.; Mir, Y.; Rouxel, C.; Brevet, D.; Basile, I.; Maynadier, M.; Vaillant, O.; Mongin, O.; Blanchard-Desce, M.; Morère, A.; Garcia, M.; Durand, J.-O.; Raehm, L. *Angew. Chem., Int. Ed.* **2011,** *50*, 11425-11429; (h) Perrier, M.; Gary-Bobo, M.; Lartigue, L.; Brevet, D.; Morère, A.; Garcia, M.; Maillard, P.; Raehm, L.; Guari, Y.;

Larinova, J.; Durand, J. O.; Mongin, O.; Blanchard-Desce, M. *J. Nanopart. Res.* **2013,** *15*, 1602; (i) Boeuf, G.; Roullin, G. V.; Moreau, J.; Van Gulick, L.; Zambrano Pineda, N.; Terryn, C.; Ploton, D.; Andry, M. C.; Chuburu, F.; Dukic, S.; Molinari, M.; Lemercier, G. *ChemPlusChem* **2014,** *79*, 171-180.

5. (a) Khurana, M.; Collins, H. A.; Karotki, A.; Anderson, H. L.; Cramb, D. T.; Wilson, B. C. *Photochem. Photobiol.* **2007,** *83*, 1441-1448; (b) Samkoe, K. S.; Clancy, A. A.; Karotki, A.; Wilson, B. C.; Cramb, D. T. *J. Biomed. Opt.* **2007,** *12*, 034025; (c) Makarov, N. S.; Drobizhev, M.; Rebane, A. *Opt. Exp.* **2008,** *16*, 4029-4047.
6. Pawlicki, M.; Collins, H. A.; Denning, R. G.; Anderson, H. L. *Angew. Chem. Int. Ed.* **2009,** *48*, 3244-3266.
7. Celli, J. P.; Spring, B. Q.; Rizvi, I.; Evans, C. L.; Samkoe, K. S.; Verma, S.; Pogue, B. W.; Hasan, T. *Chem. Rev.* **2010,** *110*, 2795-2838 and references cited therein.
8. (a) Frederiksen, P. K.; Jørgensen, M.; Ogilby, P. R. *J. Am. Chem. Soc.* **2001,** *123*, 1215-1221; (b) Nielsen, C. B.; Johnsen, M.; Arnbjerg, J.; Pittelkow, M.; McIlroy, S. P.; Ogilby, P. R.; Jorgensen, M. *J. Org. Chem.* **2005,** *70*, 7065-7079; (c) Frederiksen, P. K.; McIlroy, S. P.; Nielsen, C. B.; Nikolajsen, L.; Skovsen, E.; Jørgensen, M.; Mikkelsen, K. V.; Ogilby, P. R. *J. Am. Chem. Soc.* **2005,** *127*, 255-269.
9. Arnbjerg, J.; Paterson, M. J.; Nielsen, C. B.; Jørgensen, M.; Christiansen, O.; Ogilby, P. R. *J. Phys. Chem. A* **2007,** *111*, 5756-5767.
10. Avirah, R. R.; Jayaram, D. T.; Adarsh, N.; Ramaiah, D. *Org. Biomol. Chem.* **2012,** *10*, 911-920.
11. Arnbjerg, J.; Jiménez-Banzo, A.; Paterson, M. J.; Nonell, S.; Borrell, J. I.; Christiansen, O.; Ogilby, P. R. *J. Am. Chem. Soc.* **2007,** *129*, 5188-5199.
12. (a) Rath, H.; Sankar, J.; PrabhuRaja, V.; Chandrashekar, T. K.; Nag, A.; Goswami, D. *J. Am. Chem. Soc.* **2005,** *127*, 11608-11609; (b) Misra, R.; Kumar, R.; Chandrashekar, T. K.; Nag, A.; Goswami, D. *Org. Lett.* **2006,** *8*, 629-631.
13. (a) Drobizhev, M.; Stepanenko, Y.; Dzenis, Y.; Karotki, A.; Rebane, A.; Taylor, P. N.; Anderson, H. L. *J. Am. Chem. Soc.* **2004,** *126*, 15352-15353; (b) Kim, D. Y.; Ahn, T. K.; Kwon, J. H.; Kim, D.; Ikeue, T.; Aratani, N.; Osuka, A.; Shigeiwa, M.; Maeda, S. *J. Phys. Chem. A* **2005,** *109*, 2996-2999; (c) Ahn, T. K.; Kim, K. S.; Kim, D. Y.; Noh, S. B.; Aratani, N.; Ikeda, C.; Osuka, A.; Kim, D. *J. Am. Chem. Soc.* **2006,** *128*, 1700-1704; (d) Achelle, S.; Couleaud, P.; Baldeck, P.; Teulade-Fichou, M.-P.; Maillard, P. *Eur. J. Org. Chem.* **2011,** *2011*, 1271-1279.
14. (a) Ogawa, K.; Ohashi, A.; Kobuke, Y.; Kamada, K.; Ohta, K. *J. Am. Chem. Soc.* **2003,** *125*, 13356-13357; (b) Drobizhev, M.; Stepanenko, Y.; Rebane, A.; Wilson, C. J.; Screen, T. E. O.; Anderson, H. L. *J. Am. Chem. Soc.* **2006,** *128*, 12432-12433; (c) Ogawa, K.; Hasegawa, H.; Inaba, Y.; Kobuke, Y.; Inouye, H.; Kanemitsu, Y.; Kohno, E.; Hirano, T.; Ogura, S.-i.; Okura, I. *J. Med. Chem.* **2006,** *49*, 2276-2283.
15. Rouxel, C.; Charlot, M.; Mir, Y.; Frochot, C.; Mongin, O.; Blanchard-Desce, M. *New J. Chem.* **2011,** *35*, 1771-1780.
16. Mongin, O.; Sankar, M.; Charlot, M.; Mir, Y.; Blanchard-Desce, M. *Tetrahedron Lett.* **2013,** *54*, 6474-6478.
17. (a) Kumar, S.; Bawa, S.; Gupta, H. *Mini-Rev. Med. Chem.* **2009,** *9*, 1648-1654; (b) Solomon, V. R.; Lee, H. *Curr. Med. Chem.* **2011,** *18*, 1488-1508; (c) Kharb, R.; Kaur, H. *Int. Res. J. Pharm.* **2013,** *4*, 63-69; (d) Musiol, R. *Curr. Pharm. Des.* **2013,** *19*, 1835-1849; (e) Mukherjee, S.; Pal, M. *Drug Discov. Today* **2013,** *18*, 389-398; (f) Gryzlo, B.; Kulig, K. *Mini-Rev. Med. Chem.* **2014,** *14*, 332-344.
18. (a) Morten, A. G.; Martinez, L. J.; Holt, N.; Sik, R. H.; Reszka, K.; Chignell, C. F.; Tonnesen, H. H.; Roberts, J. E. *Photochem. Photobiol.* **1999,** *69*, 282-287; (b) Navaratnam, S.; Hamblett, I.; Tonnesen, H. H. *J. Photochem. Photobiol. B Biol.* **2000,** *56*, 25-38.
19. (a) Shavaleev, N. M.; Adams, H.; Best, J.; Edge, R.; Navaratnam, S.; Weinstein, J. A. *Inorg. Chem.* **2006,** *45*, 9410-9415; (b) Zhou, C.-H.; Zhao, X. *J. Organomet. Chem.* **2011,** *696*, 3322-3327; (c) Pefkianakis, E. K.; Christodouleas, D.; Giokas, D. L.; Papadopoulos, K.; Vougioukalakis, G. C. *Eur. J. Inorg. Chem.* **2013,** *2013*, 4628-4635; (d) Ashen-Garry, D.; Selke, M. *Photochem. Photobiol.* **2014,** *90*, 257-274.
20. Marco-Contelles, J.; Pérez-Mayoral, E.; Samadi, A.; Carreiras, M. d. C.; Soriano, E. *Chem. Rev.* **2009,** *109*, 2652-2671.
21. Alabaster, C. T.; Bell, A. S.; Campbell, S. F.; Ellis, P.; Henderson, C. G.; Roberts, D. A.; Ruddock, K. S.; Samuels, G. M. R.; Stefaniak, M. H. *J. Med. Chem.* **1988,** *31*, 2048-2056.
22. Ganzha, V. A.; Gurinovich, G. P.; Dzhagarov, B. M.; Egorova, G. D.; Sagun, E. I.; Shul'ga, M. *J. Appl. Spectrosc.* **1989,** *50*, 402-406.
23. Xu, C.; Webb, W. W. *J. Opt. Soc. Am. B* **1996,** *13*, 481-491.
24. (a) Rouxel, C.; Charlot, M.; Mongin, O.; Krishna, T. R.; Caminade, A.-M.; Majoral, J.-P.; Blanchard-Desce, M. *Chem. Eur. J.* **2012,** *18*, 16450-16462; (b) Picard, S.; Genin, E.; Clermont, G.; Hugues, V.; Mongin, O.; Blanchard-Desce, M. *New J. Chem.* **2013,** *37*, 3899-3913.
25. (a) Kelkar, S. S.; Reineke, T. M. *Bioconjugate Chem.* **2011,** *22*, 1879-1903; (b) Couleaud, P.; Bechet, D.; Vanderesse, R.; Barberi-Heyob, M.; Faure, A.-C.; Roux, S.; Tillement, O.; Porhel, S.; Guillemin, F.; Frochot, C. *Nanomedicine* **2011,** *6*, 995-1009; (c) Benachour, H.; Seve, A.; Bastogne, T.; Frochot, C.; Vanderesse, R.; Jasniewski, J.; Miladi, I.; Billotey, C.; Tillement, O.; Lux, F.; Barberi-Heyob, M. *Theranostics* **2012,** *2*, 889-904; (d) Truillet, C.; Lux, F.; Moreau, J.; Four, M.; Sancey, L.; Chevreux, S.; Boeuf, G.; Perriat, P.; Frochot, C.; Antoine, R.; Dugourd, P.; Portefaix, C.; Hoeffel, C.; Barberi-Heyob, M.; Terryn, C.; van Gulick, L.; Lemercier, G.; Tillement, O. *Dalton Trans.* **2013,** *42*, 12410-12420; (e) Gibot, L.; Lemelle, A.; Till, U.; Moukarzel, B.; Mingotaud, A.-F.; Pimienta, V.; Saint-Aguet, P.; Rols, M.-P.; Gaucher, M.; Violleau, F.; Chassenieux, C.; Vicendo, P. *Biomacromolecules* **2014,** *15*, 1443-1455.
26. (a) Demas, J. N.; Crosby, G. A. *J. Phys. Chem.* **1971,** *75*, 991-1024; (b) Eaton, D. F. *Pure Appl. Chem.* **1988,** *60*, 1107-1114.
27. (a) Albota, M. A.; Xu, C.; Webb, W. W. *Appl. Opt.* **1998,** *37*, 7352-7356; (b) Katan, C.; Tretiak, S.; Werts, M. H. V.; Bain, A. J.; Marsh, R. J.; Leonczek, N.; Nicolaou, N.; Badaeva, E.; Mongin, O.; Blanchard-Desce, M. *J. Phys. Chem. B* **2007,** *111*, 9468-9483.
28. Werts, M. H. V.; Nerambourg, N.; Pélégry, D.; Le Grand, Y.; Blanchard-Desce, M. *Photochem. Photobiol. Sci.* **2005,** *4*, 531-538.

8-Br-quinolines derivatives as sensitizers combining two-photon induced fluorescence and singlet oxygen generation.

Sébastien Picard, Guillaume Clermont, Emilie Genin, Mireille Blanchard-Desce*

Univ. Bordeaux, Institut des Sciences Moléculaires, CNRS UMR 5255, 351 cours de la Libération, F-33405 Talence Cedex, France

∗ Corresponding author. Tel.: +33 5 40 00 67 32; fax: +33 5 40 00 69 94.
E-mail address: m.blanchard-desce@ism.u-bordeaux1.fr

Table of Contents

[1]H and [13]C NMR spectra

2-amino-3-bromo-5-((4-(diphenylamino)phenyl)ethynyl)benzaldehyde (5)

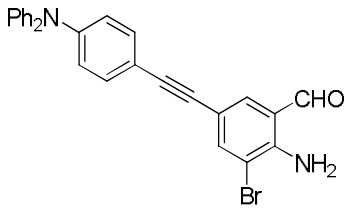

^{1}H NMR (200 MHz, $CDCl_3$)

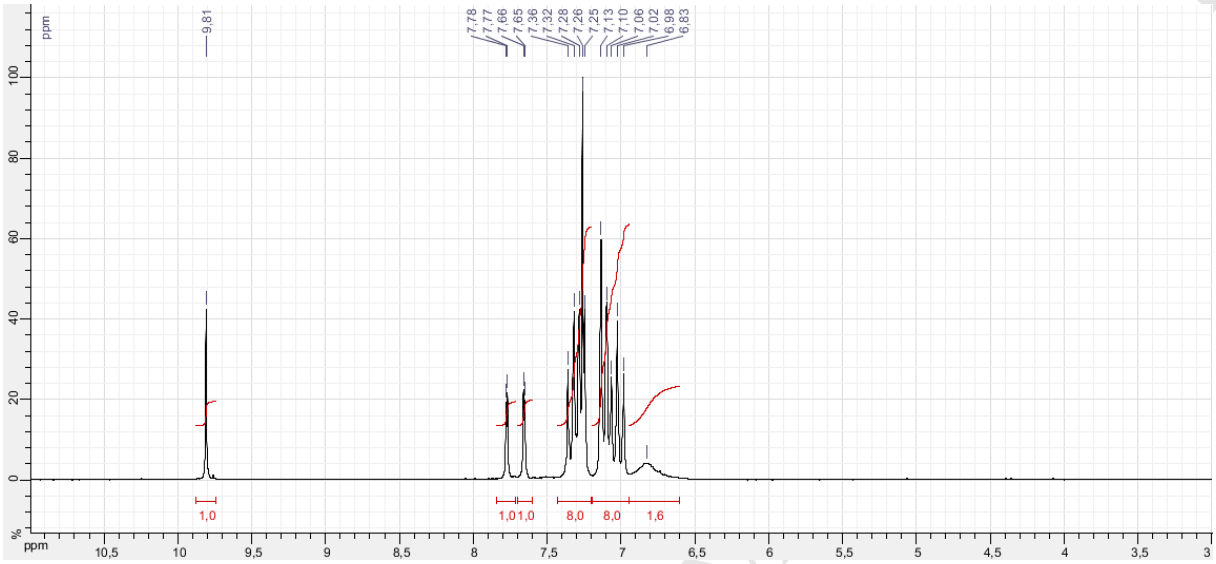

^{13}C NMR (50 MHz, $CDCl_3$)

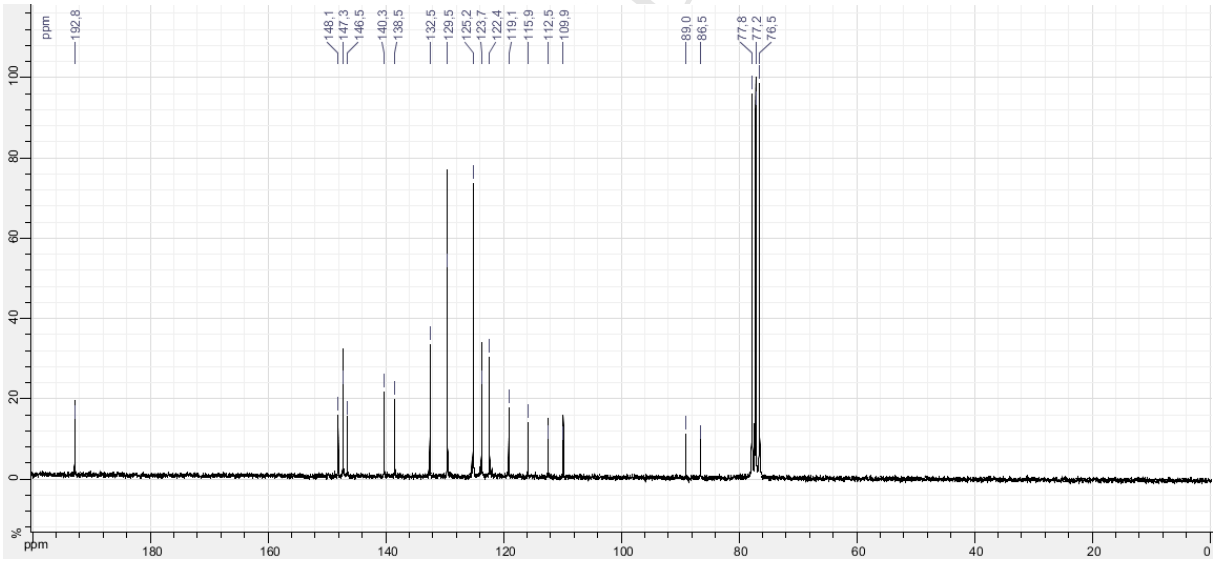

4-((8-bromo-2-methylquinolin-6-yl)ethynyl)-*N*,*N*-diphenylaniline (6)

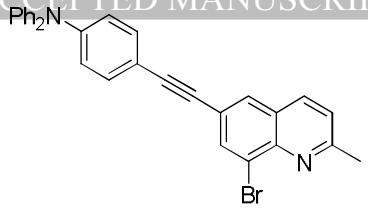

^{1}H NMR (200 MHz, $CDCl_3$)

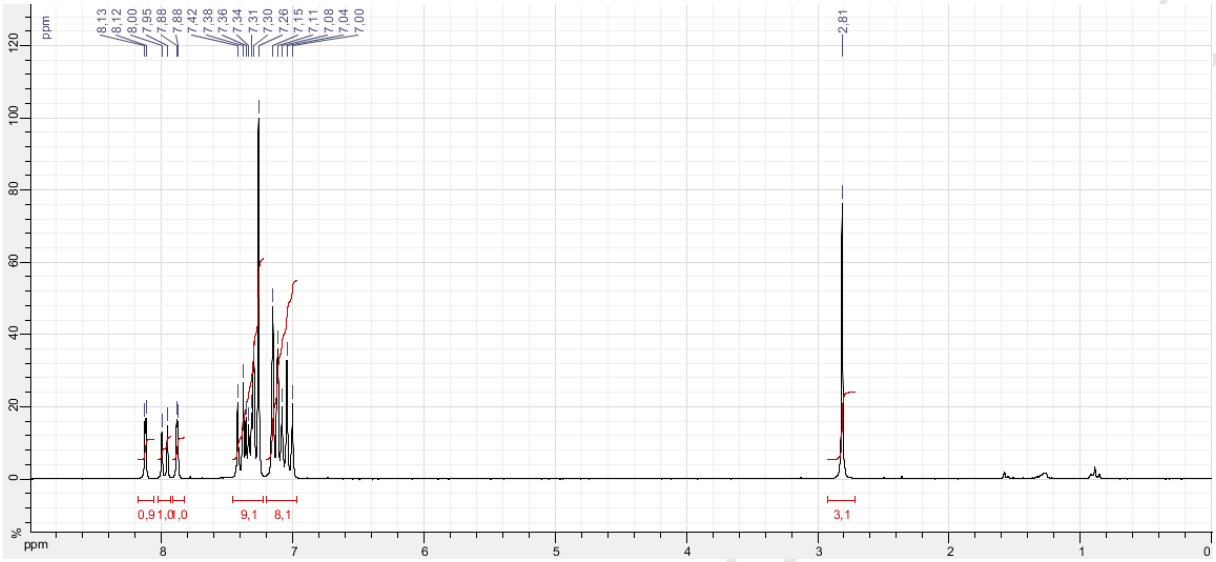

^{13}C NMR (50 MHz, $CDCl_3$)

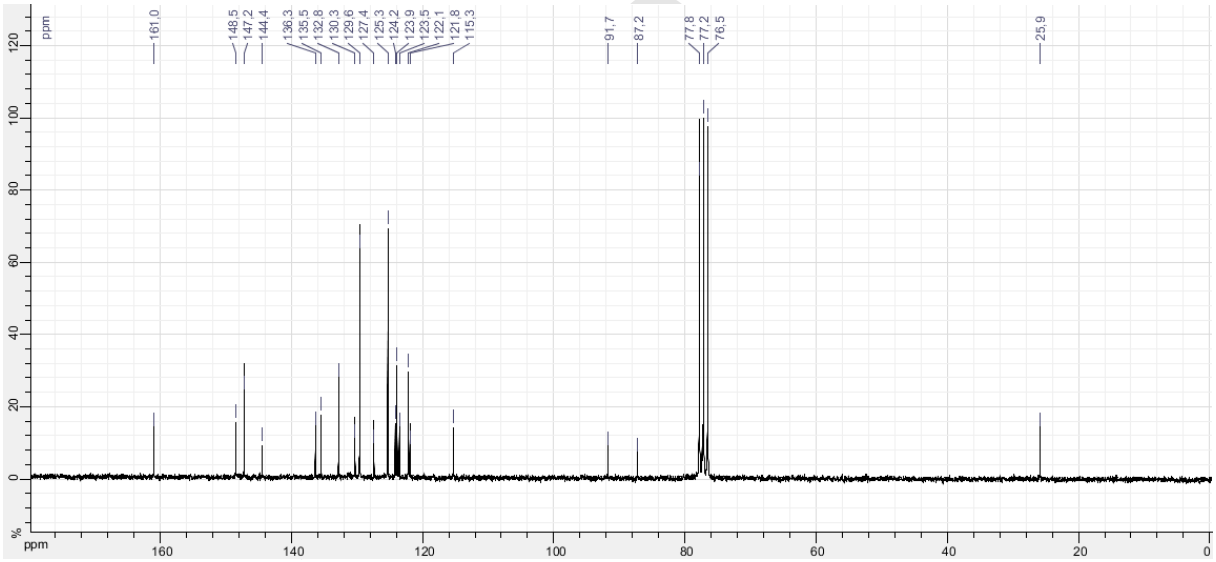

8-bromo-6-((4-(diphenylamino)phenyl)ethynyl)quinoline-2-carbaldehyde (7)

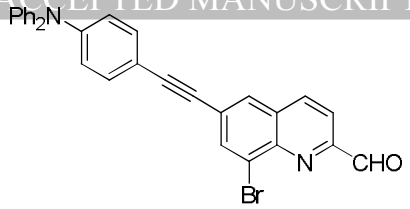

^{1}H NMR (200 MHz, $CDCl_3$)

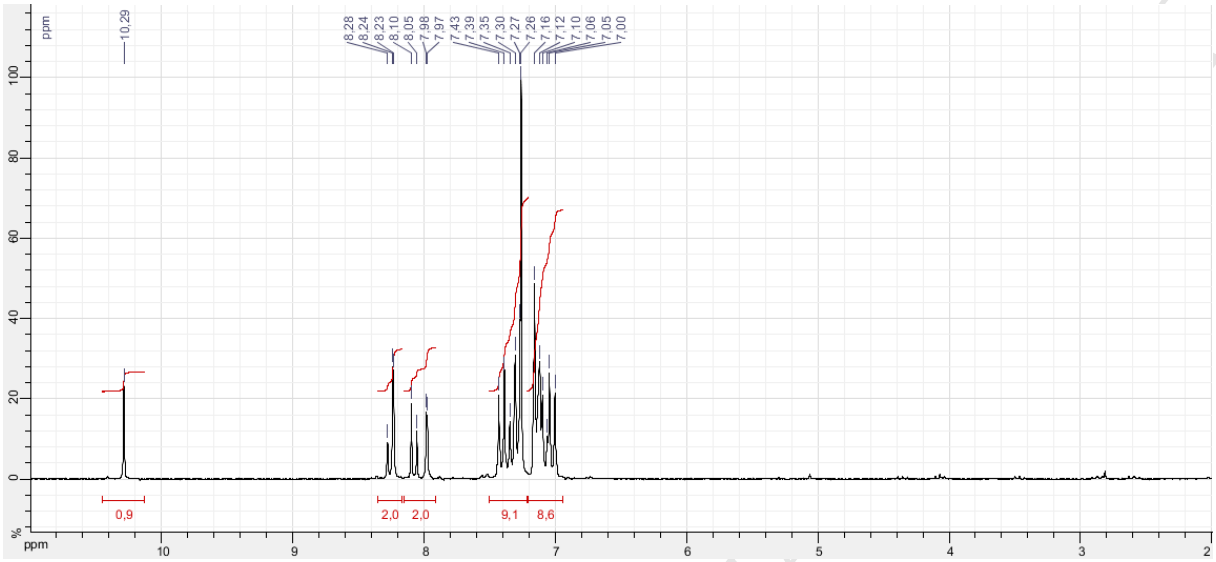

^{13}C NMR (50 MHz, $CDCl_3$)

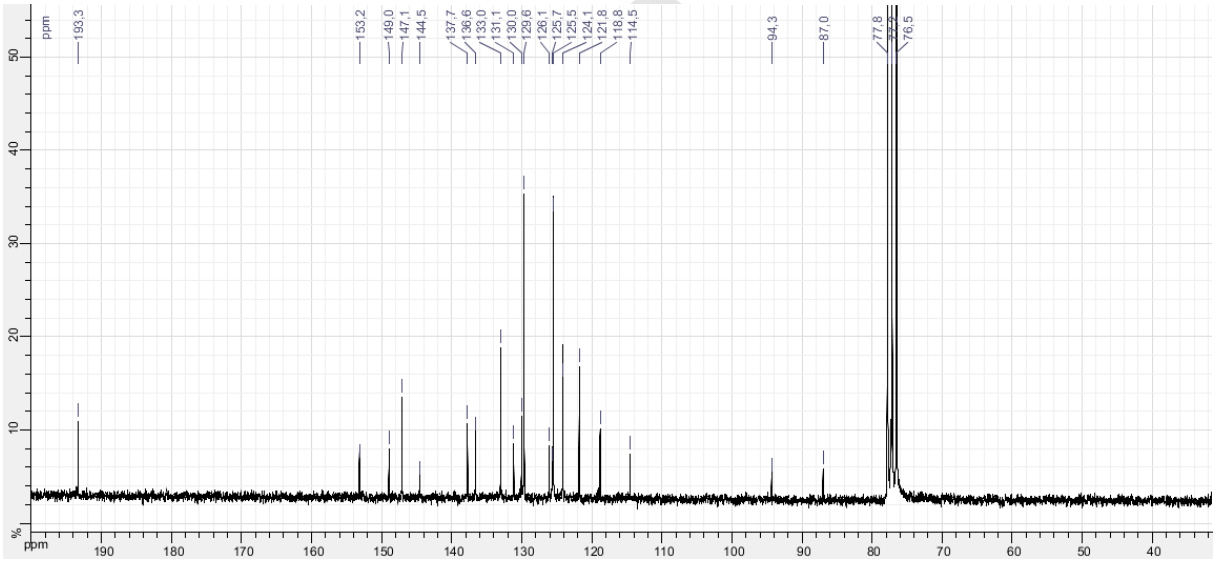

(8-bromo-6-((4-(diphenylamino)phenyl)ethynyl)quinolin-2-yl)methanol (8)

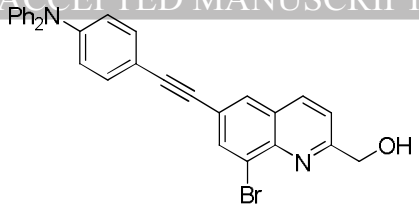

^{1}H NMR (200 MHz, $CDCl_3$)

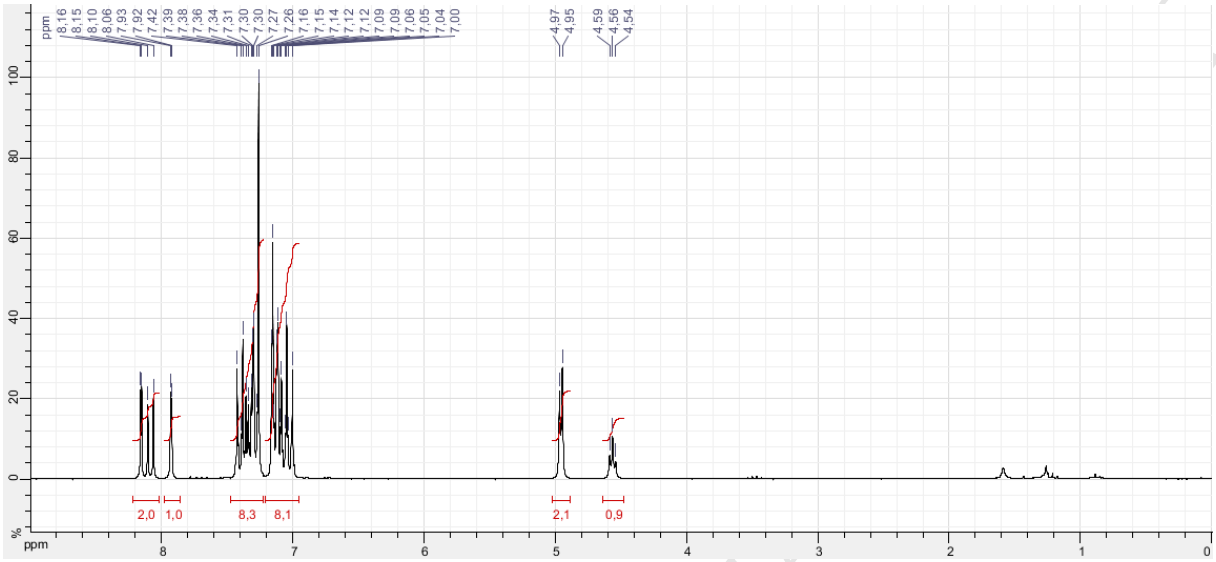

^{13}C NMR (50 MHz, $CDCl_3$)

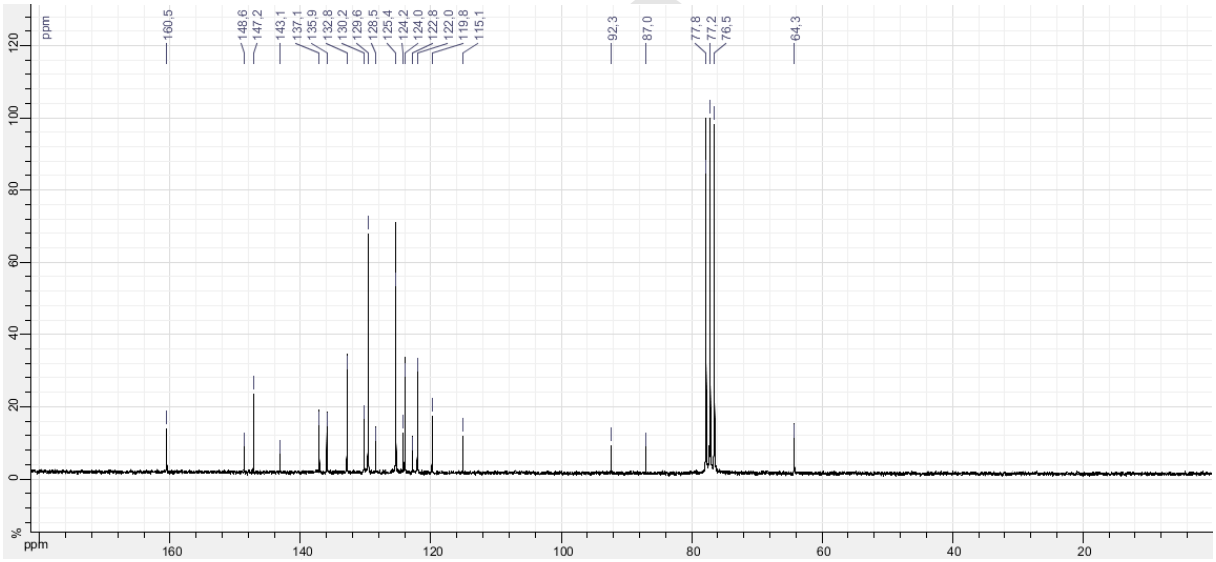

8-bromo-6-((4-(diphenylamino)phenyl)ethynyl)-2-methylquinolin-3-ol (10)

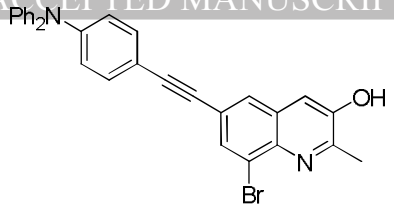

^{1}H NMR (600 MHz, DMSO-d_6)

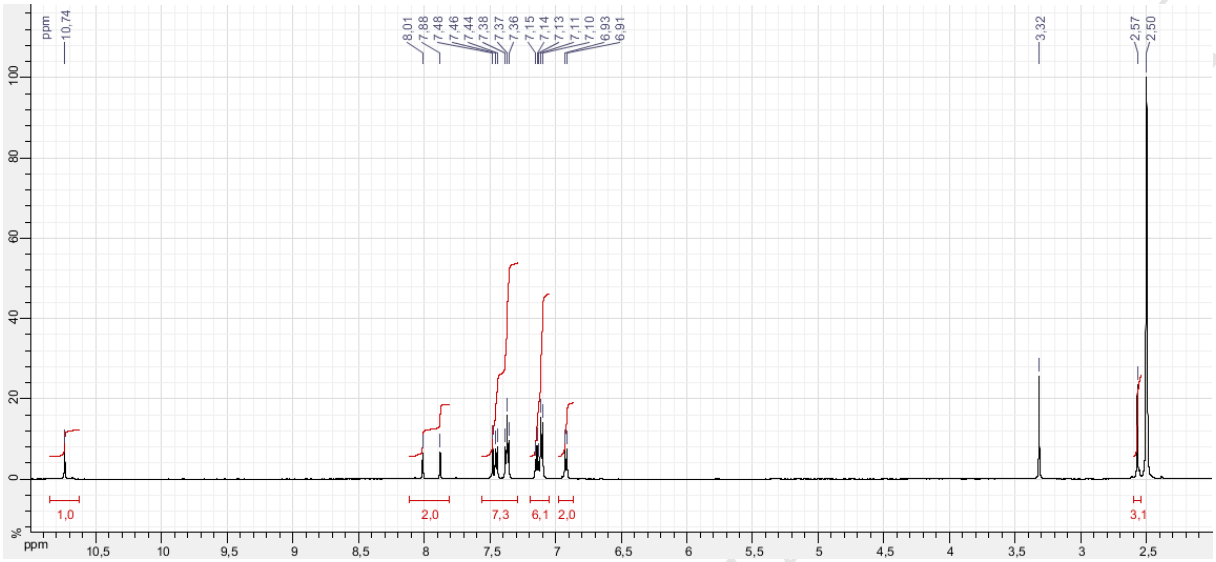

^{13}C NMR (50 MHz, DMSO-d_6)

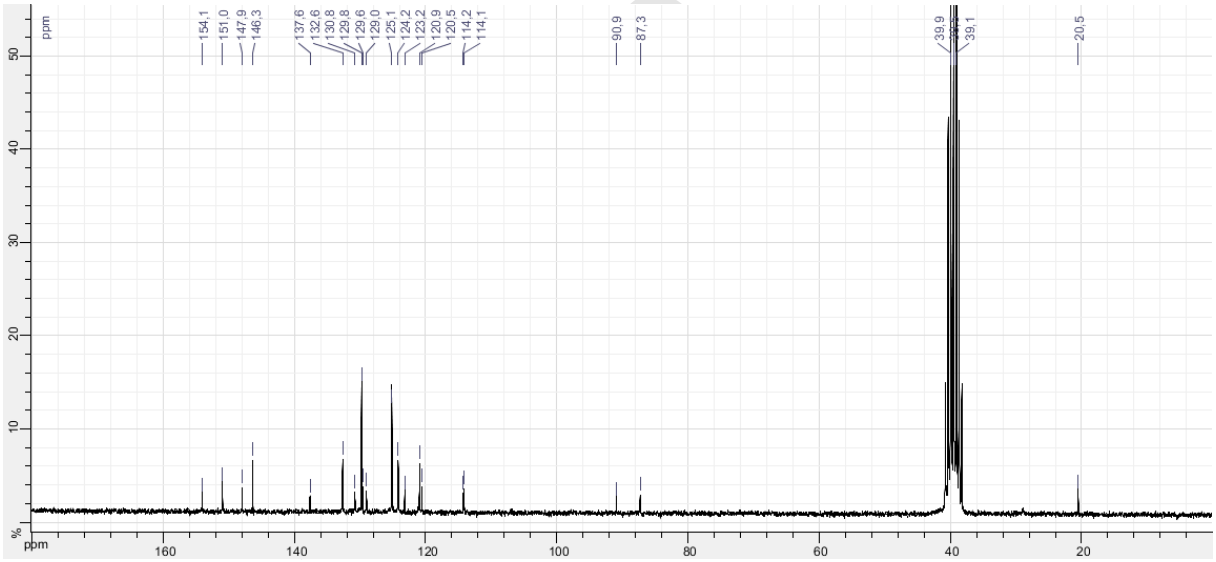

8-bromo-6-((4-(diphenylamino)phenyl)ethynyl)-2-(hydroxymethyl)quinolin-3-ol (12)

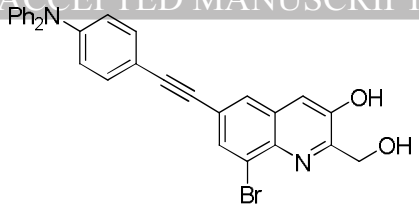

^{1}H NMR (200 MHz, DMSO-d_6)

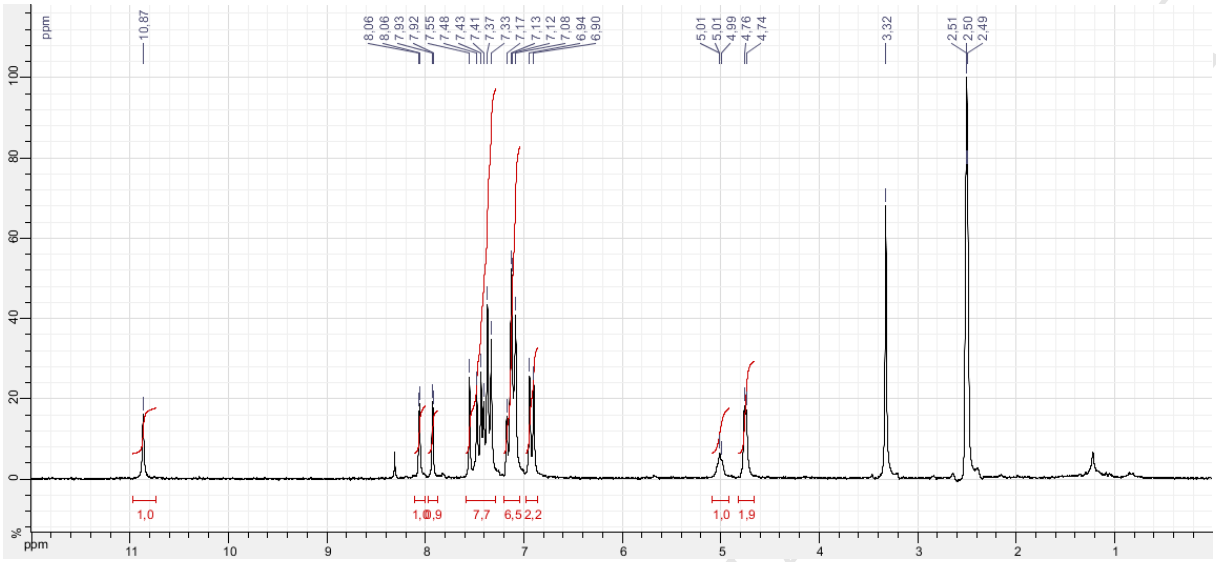

^{13}C NMR (50 MHz, DMSO-d_6)

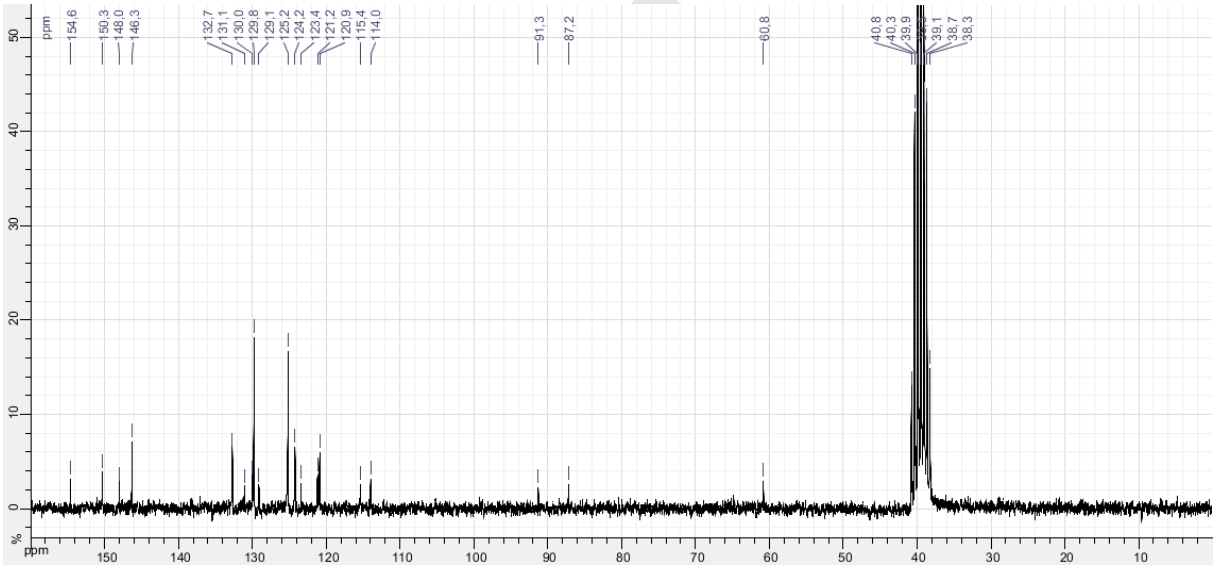

Solvatochromic data

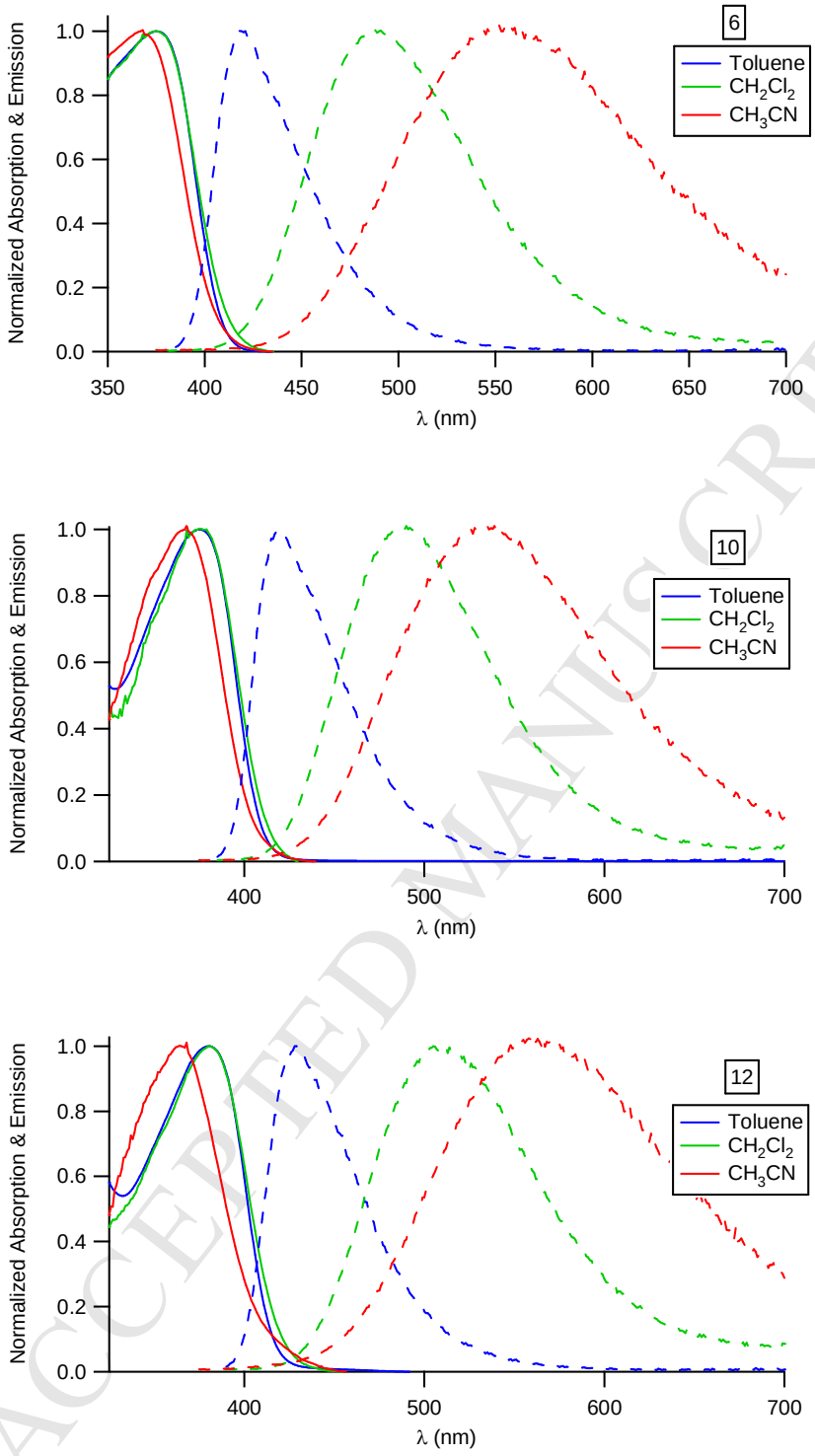

Figure S1. Absorption and emission spectra of compounds **6**, **10**, **12** in solvents of different polarities.

Two-photon absorption data

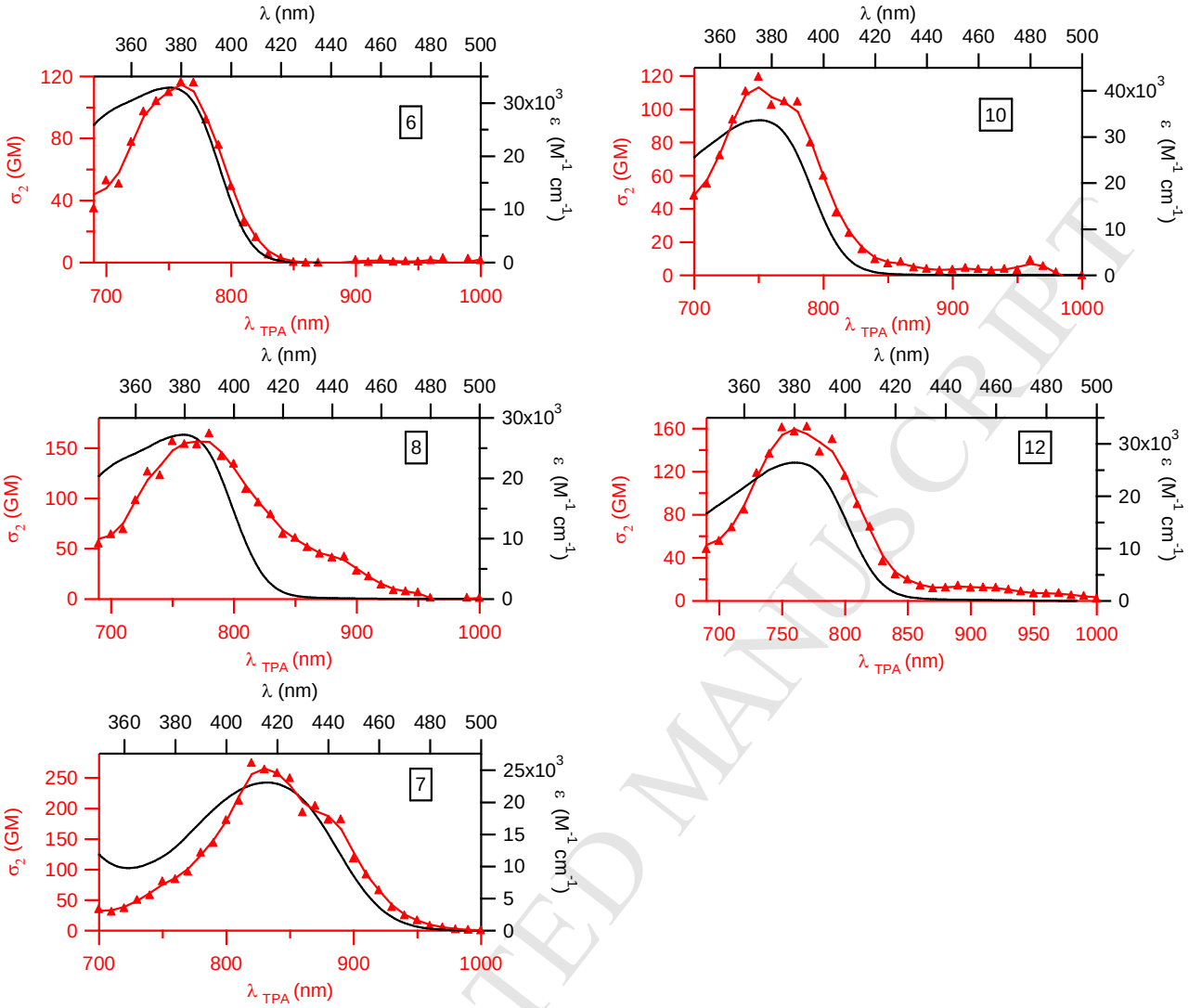

Figure S2. Compared one-photon absorption (black line) and two-photon absorption (red line) spectra of compounds **6**-**8**, **10**, **12** in toluene.